Non-iterative Computation of Contact Forces for Deformable Objects

J. Spillmann M. Becker M. Teschner

Computer Graphics
University of Freiburg, Germany

ABSTRACT

We present a novel approach to handle collisions of deformable objects represented by tetrahedral meshes. The scheme combines the physical correctness of constraint methods with the efficiency of penalty approaches.
For a set of collided points, a collision-free state is computed that is governed by the elasticities and impulses of the collided objects. In contrast to existing constraint methods we show how to decouple the resulting system of equations in order to avoid iterative solvers.
By considering the time step of the numerical integration scheme, the contact force can be analytically computed for each collided point in order to achieve the collision-free state. Since predicted information on positions, impulses, and penetration depths of the subsequent time step is considered, a collision-free state is maintained at each simulation step which is in contrast to existing penalty methods. Further, our approach does not require a user-defined stiffness constant.
Our scheme can handle various underlying deformable models and numerical integration schemes. To illustrate its versatility, we have performed experiments with linear and non-linear finite element methods.

Keywords: Physically-based animation, Collision response, Contact forces, Deformable modeling

1 INTRODUCTION

Contact handling for deformable objects provides unique challenges since the surfaces in the contact region deform due to emerging contact forces. This induces quickly alternating stress onto the contact regions, which must be considered for each contact point separately.

There exist two classes of schemes to handle collisions of deformable objects. *Penalty methods* relate the magnitude of the response force to an interpenetration measure. Apart from the fact that this lacks physical plausibleness, these approaches require the definition of a stiffness constant k for each collision. k must be large enough to resolve the collision entirely without overshooting, even for large stresses onto the collided points. Considering that the stress varies spatially and temporally, the choice of k is intrinsically difficult. *Constraint methods* impose non-penetration constraints for all contact points in order to compute response forces or impulses. Schemes have been proposed that formulate e. g. a linear complementary problem (LCP) or employ Lagrange multipliers. To solve the resulting system of equations, iterative methods are employed. Thus, the resulting methods tend to be expensive or sensitive to numerical problems and require moreover effortful implementations.

Our contribution. We present a novel scheme for handling collisions of deformable objects. Our approach combines the accuracy and physical correctness of constraint methods with the simplicity and efficiency of penalty methods.

To identify the collision-free positions of the collided points, we establish a linearized relation between the internal force and the displacement of each point. We then show how to decouple the resulting system of equations such that it can be solved analytically, i. e. without employing iterative methods. Though the resulting contact forces are approximative, energy conservation is guaranteed. The contact forces correct the unconstrained motion of the mass points, maintaining a collision-free state at each simulation step.

In summary, our approach comprises the following advantages over previous approaches:

- In contrast to previous constraint methods, the system of equations is decoupled and can be solved analytically, requiring only a small and constant number of operations per contact point. It is thus less vulnerable to numerical problems and enables a simple and elegant implementation. Further, our approach can handle various underlying deformable models.

- In contrast to previous penalty methods, we do not require the definition of response constants. The magnitude of the response forces depends on the positions, impulses and internal forces of the collided points. As a consequence, spatially and temporally varying elasticity can be handled correctly. Further, a collision-free state is maintained in each simula-

tion step since colliding points are accelerated onto the contact surface within one integration step.

Several experiments have been performed that underline the conceptual advantages of our approach (see Fig. 1). To show that the proposed approach can handle various deformable models, both linear and non-linear finite element (FE) methods, and a mass-spring deformable model are employed.

2 RELATED WORK

In this work, we focus on the contact dynamics of deformable objects. Pioneering work on deformable objects in computer graphics has been done by Terzopoulos [TPBF87], and a recent survey on the simulation of deformable objects is [NMK*05]. In [TKH*05], the state-of-the-art of the collision detection of deformable objects is summarized. Two different classes of collision response methods can be identified, notably penalty and constraint methods.

Penalty methods compute a response force per collided point whose magnitude is related to an interpenetration measure. As a consequence, the numerical effort grows with the violence of penetration, as first mentioned by Moore [MW88]. Further, penalty methods require a robust and concise computation of the penetration depth of collided points. This problem is amongst others identified by Hirota et al. [HFS03] in the context of objects deformed with FE methods. They state that discontinuities lead to oscillations, and thus they propose to compute smooth contact normals by employing a distance field. However, the accuracy of this scheme is limited since the distance field is not updated upon deformation. Later, Heidelberger et al. [HTK*04] proposed to compute smooth contact normals from a set of closest surface features. We employ this scheme to compute the contact normals since it provides good accuracy and robustness at minor computational effort.

In contrast to traditional penalty methods, we consider the impulses and elasticities of colliding objects when computing the contact forces. We compute the position of a collided point on the contact surface, and then apply a force to the point that accelerates it immediately to this position. Keiser et al. [KMH*04] proposed a similar scheme for meshless objects. They compute a virtual contact surface based on the ratio of elasticities of the objects. However, they do not describe how to cope with collisions at different impulses. Further, they still require the definition of a response force constant. Recently, it has been shown that penalty-based collision response can also be applied to level-of-detail representations [DMG05].

Constraint methods usually define a system of non-penetration constraints. This system is formulated as a linear complementary problem (LCP). The contact forces are then computed by solving the system. Constraint methods are particularly interesting in rigid-body dynamics, since rigid bodies provide less degrees-of-freedom. An excellent work on collision handling of rigid bodies has recently been presented by Kaufman et al. [KEP05] that is based on the pioneering work of Moreau [Mor88]. They especially introduce a friction model that leads to a separable quadratic program.

Constraint-based collision response of deformable objects is first discussed in 1992. Baraff and Witkin [BW92], based on the work of Baraff [Bar89], use a variational principle to compute impulses that prevent interpenetration. However, their underlying deformable model is not physically motivated. Their approach is extended by Gascuel [Gas93] by computing an exact contact surface described by deformation fields. Her approach clearly parallels ours in respect of the formulation of non-penetrance. However, the application of implicit functions to define the surfaces obviously imposes limitations.

With growing computational power, approaches that simulate deformable objects as systems of mass points received increasing attention. An approach that handles collisions between objects deformed by FE methods is presented by Debunne et al. [DDCB01]. The approach implements non-penetration constraints by directly displacing collided vertices. While this technique works well for handling collisions between rigid haptic tools and deformable objects, it lacks physical plausibleness.

A large step towards physically based collision handling is done by Duriez et al. [DDKA06]. They solve an LCP based on Signorini's contact theory [DAK04]. The link between contact forces and point displacements is established by a compliance matrix which assumes a linear or linearized deformation around the contact point. Pauly et al. [PPG04] model contact resolution for quasi-rigid objects. Their work parallels our approach since they also compute a contact surface based on constraints, and then derive forces that accelerate the points onto this surface. However, similar to Duriez et al., their approach depends on the deformation model. Moreover, they explicitly enforce volume preservation. Further, Pauly et al. maintain a pressure equilibrium which applies only to static configurations, while we enforce a contact force equilibrium that applies to dynamic configurations. In addition, our approach treats the deformable model as a black box. We can thus not only handle objects deformed with linear or non-linear FE methods, but also objects simulated as mass-spring meshes.

A comparison between penalty and constraint methods is presented by Hauser et al. [HSO03]. They state that penalty methods are faster while constraint methods provide more robustness and allow for larger time steps. However, they also state that solving the system of constraints is not always possible in real-time. We present a way to solve a system of constraints analytically, i. e. without employing iterative methods.

Recently, a promising approach was presented by Galoppo et al. [GOM*06]. They model objects with a rigid core overlaid by a deformation texture (see also [JP02]). The collision response is induced by applying impulses. The approach produces plausible deformations at good performance. However, the pro-

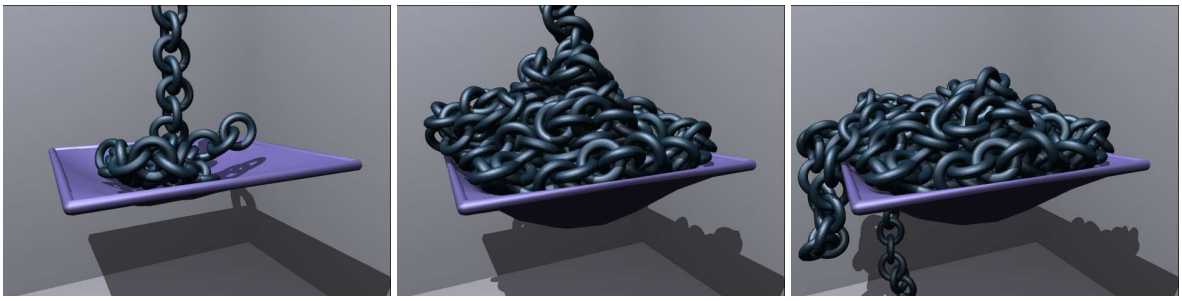

Figure 1: Simulation of 200 chained torii falling onto an elastic membrane. The membrane deforms and buckles under the weight of the chain. Nevertheless, a stable resting state is reached using the proposed collision response scheme.

posed Sherman-Morrison-Woodbury update to resolve the system of constraints is not always stable [Hig96]. In contrast, we propose a direct method that is less vulnerable to numerical problems. The idea to handle collision response for deformable objects by applying impulses is also mentioned in a recent publication of Cirak [CW05]. Here, the velocities of the points are changed by impulses, while the colliding points are directly displaced in order to achieve a collision-free setting. However, as shown in [ST05], the direct displacement of primitives can influence the stability of the simulation since it violates the laws of dynamics with respect to inertia. In contrast, we compute a constrained force that accelerates a mass point onto a collision-free position.

3 METHOD

We assume that the deformable objects are discretized into tetrahedral meshes, and that the surfaces of the objects are triangulated. We further assume that all n simulated mass points have a mass larger than zero.

For the following discussion, we assume that the objects have been numerically evolved in time, resulting in unconstrained positions $\tilde{\mathbf{x}}_i^{t+\Delta t}$. For each colliding point in the set C of colliding points, a penetration vector $\mathbf{d}_i^{t+\Delta t}$ has been computed [HTK*04]. Further, we treat only the case where two colliding objects share a single contact region. However, the generalization to multiple simultaneously colliding objects is straight forward.

We now show how to compute contact forces that correct the previous unconstrained motion. The contact forces, applied at time t, result in constrained positions $\mathbf{x}_i^{t+\Delta t}$.

3.1 Terms

A *collision* is a pair (i,T_i), where $i \in C$ is a point that has collided with a volume under unconstrained motion. $T_i = \{j,k,l\}$ is the triangle on the surface of the collided object that has been penetrated by i. We denote i consistently as *contact point*.

In the following discussion, we assume that all vertices $j \in T_i$ of a collision (i,T_i) are colliding themselves. The boundary cases where not all vertices of T_i are in C are omitted due to lack of space.

The *mapping matrix* $\mathbf{H} = (h_{ij}) \in \mathbb{R}^{n \times n}$ provides the barycentric coordinates $\omega_{i,j}$ of the point i projected onto T_i with respect to $j \in T_i$ (see Fig. 2):

$$h_{ij} = \begin{cases} \omega_{i,j} & j \in T_i \\ 0 & \text{else} \end{cases}$$

with $\sum_{j=1}^{n} h_{ij} = 1$ for all i. $\mathbf{H}$ can easily be obtained from the penetration directions $\mathbf{d}_i^{t+\Delta t}$. Notice that $\mathbf{H}$ is required for the derivation of the contact forces, but it is not explicitly represented in the actual implementation.

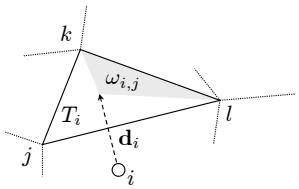

Figure 2: The element h_{ij} provides the barycentric coordinate $\omega_{i,j}$ of the contact point i projected onto the penetrated surface triangle T_i with respect to $j \in T_i$.

Each collision (i,T_i) induces a *local force* $\mathbf{f}_i$ on the point i and local forces $\mathbf{f}_{T_i}$ on the vertices of T_i. In general, each vertex j, k and l will itself be involved in collisions, and each of these collisions induces local forces. As a consequence, multiple local forces act on the same contact point. This intrinsic coupling of collisions results in conflicting constraints that make the computation of contact forces difficult, as e. g. mentioned by Volino et al. [VMT00].

The *contact force* $\mathbf{F}_i$ is the sum of all local forces $\mathbf{f}_i$ and $\mathbf{f}_{T_j}$ with $i \in T_j$, acting on the point i.

3.2 Contact mechanics

Newton's third law states that for two entities in contact, the force that the first entity exerts on the second entity must be opposite equal to the force exerted by the second entity on the first entity. As a consequence, the sum of contact forces must always be 0. We denote this situation as *force equilibrium*.

This does not imply that the stresses of the deformed volumes sum to 0. In fact, this condition only holds for static configurations, so-called resting contacts (see e. g. [PPG04]). Following Newton, there is an equilibrium of the local forces induced by a collision (i, T_i)

$$\mathbf{f}_i + \mathbf{f}_{T_i} = 0 \tag{1}$$

The global force equilibrium states that the sum of all contact forces must be 0.

$$\sum_{i \in C} \mathbf{F}_i = 0 \tag{2}$$

The global force equilibrium guarantees energy conservation during the collision.

3.3 Contact forces

In order to decouple the contact force computations per collision, we assume that the contact space per collision (i, T_i) is spanned by $\mathbf{d}_i^{t+\Delta t}$. Thus, we assume that the penetration depths of points j, k and $l \in T_i$ conform to the penetration depth of point i:

$$\mathbf{d}_j^{t+\Delta t} = \mathbf{d}_k^{t+\Delta t} = \mathbf{d}_l^{t+\Delta t} = -\mathbf{d}_i^{t+\Delta t} \tag{3}$$

However, this assumption introduces an error. In Sec. 3.5 we show how to minimize the impact of this error. As a consequence of (3), each collision defines its own contact space, and thus a contact point has multiple penetration depths, notably one for each collision that it is involved into.

The collision-free position $\mathbf{x}_i^{t+\Delta t}$ lives in the contact space of the collision (i, T_i). Since the contact space of (i, T_i) has dimension one, the computation of the collision-free position $\mathbf{x}_i^{t+\Delta t}$ reduces to finding a scalar $\alpha \in [0,1]$ with $\mathbf{x}_i^{t+\Delta t} = \tilde{\mathbf{x}}_i^{t+\Delta t} + \alpha \mathbf{d}_i^{t+\Delta t}$.

Claim:

By applying a contact force

$$\mathbf{F}_i = \frac{m_i}{\Delta t^2} \mathbf{d}_i^{t+\Delta t} \alpha_i \tag{4}$$

with

$$\alpha_i = \frac{\sum_{j=1}^n c_j h_{ij} m_j}{c_i m_i + \sum_{j=1}^n c_j h_{ij} m_j} \tag{5}$$

and constants

$$c_i = \frac{1}{1 + \sum_{j=1}^n h_{ji}} \tag{6}$$

to a contact point at current position $\mathbf{x}_i^t$, the unconstrained motion is corrected and the point is accelerated onto the collision-free position $\mathbf{x}_i^{t+\Delta t}$. Further, the computed contact forces meet both (1) and (2). The collision-free positions $\mathbf{x}_i^{t+\Delta t}$ are given by

$$\mathbf{x}_i^{t+\Delta t} = \tilde{\mathbf{x}}_i^{t+\Delta t} + \alpha_i \mathbf{d}_i^{t+\Delta t} \tag{7}$$

Notice that $\sum_{j=1}^n h_{ij}$ sums over all vertices of the compliant triangle T_i of the contact point i. In contrast, $\sum_{j=1}^n h_{ji}$ sums over all occurrences of point $i \in T_j$, which conforms to the sum of the barycentric coordinates of all points j that have penetrated a triangle adjacent to point i.

An amortized analysis shows that the weights c_i can be computed per contact point at constant costs. Thus the costs to compute $\mathbf{F}_i$ per point are constant.

Rationale:

To motivate the proposed contact forces, three aspects have to be explained, notably that the proposed constrained positions are collision-free, that the collision-free state is immediately obtained, and that the contact forces obey the Newtonian laws of force equilibrium.

3.3.1 Collision-free state

We claimed that the positions $\tilde{\mathbf{x}}_i^{t+\Delta t} + \alpha_i \mathbf{d}_i^{t+\Delta t}$ define a collision-free state. We assumed that the collision-free position of the contact point lives in the contact space spanned by $\mathbf{d}_i^{t+\Delta t}$, and that the penetration depths of the vertices $j \in T_i$ conform to the penetration depth of i. Thus, we have to show that $\alpha_i + \alpha_j \approx 1$ for all $j \in T_i$.

Consider the sum $\sum_{j=1}^n c_j h_{ij} m_j$ in the numerator of the expression (5) for α_i. We interpret this sum as a mass averaging operation over vertices j on the opposite surface. We thus define the average mass $\overline{m}_j$ of vertices j as

$$\sum_{j=1}^n c_j h_{ij} m_j = \overline{m}_j \sum_{j=1}^n h_{ij} c_j \tag{8}$$

The row sums $\sum_{j=1}^n h_{ij}$ of the mapping matrix $\mathbf{H}$ equal 1 per definition. Thus, the average of the column sums $\sum_{j=1}^n h_{ji}$ of $\mathbf{H}$ is also 1, and we therefore approximate $c_j \approx \frac{1}{2}$. This approximation allows to rewrite α_i of the contact point as

$$\alpha_i = \frac{\overline{m}_j/2}{m_i/2 + \overline{m}_j/2} \tag{9}$$

Now consider a point $j \in T_i$. The α_j of this point is

$$\alpha_j = \frac{\overline{m}_k/2}{m_j/2 + \overline{m}_k/2} \tag{10}$$

with $\overline{m}_k$ the average mass of points in the compliant surface triangle opposite to j and thus in the neighborhood of i. By assuming that the differences in the masses of neighboring vertices are small, we approximate $\overline{m}_k \approx m_i$ and $\overline{m}_j \approx m_j$. Thus the sum of α_i and α_j is

$$\alpha_i + \alpha_j \approx \frac{m_j/2}{m_i/2 + m_j/2} + \frac{m_i/2}{m_j/2 + m_i/2} = 1 \tag{11}$$

Notice that this does not restrict the masses of the colliding objects to be equal. In fact, the expression for α_i ensures that collisions of objects at differing weights are handled correctly, which is in contrast to penalty methods. Further, the objects may have spatially differing masses.

We conclude that the proposed constrained positions $\mathbf{x}_i^{t+\Delta t}$ yield a collision-free state. In Sec. 3.5 we discuss under which circumstances the errors induced by the approximation are minimized.

3.3.2 Obtaining the goal position

To show that by applying the proposed contact forces $\mathbf{F}_i$ to points at $\tilde{\mathbf{x}}_i^{t+\Delta t}$, the collision-free positions $\mathbf{x}_i^{t+\Delta t}$ are immediately reached, we linearize the relation between internal force and displacement at the current time step. This allows to relate the contact force to the penetration depth of the collided point. We then integrate the sum $\mathbf{p}_i + \mathbf{F}_i$ of the known internal force $\mathbf{p}_i$ and the unknown contact force $\mathbf{F}_i$ of the point numerically. Thereby, we employ the Verlet scheme:

$$\begin{aligned} \mathbf{x}_i^{t+\Delta t} &= 2\mathbf{x}_i^t - \mathbf{x}_i^{t-\Delta t} + \frac{\Delta t^2}{m_i}(\mathbf{p}_i + \mathbf{F}_i) \\ &= 2\mathbf{x}_i^t - \mathbf{x}_i^{t-\Delta t} + \frac{\Delta t^2}{m_i}\mathbf{p}_i + \frac{\Delta t^2}{m_i}\mathbf{F}_i \\ &= \tilde{\mathbf{x}}_i^{t+\Delta t} + \frac{\Delta t^2}{m_i}\mathbf{F}_i \end{aligned} \tag{12}$$

In (12), we relate the constrained position $\mathbf{x}_i^{t+\Delta t}$ to the contact force $\mathbf{F}_i$. The internal force $\mathbf{p}_i$ on the point is implicitly considered in the unconstrained position $\tilde{\mathbf{x}}_i^{t+\Delta t}$. The constrained position is given by (7):

$$\mathbf{x}_i^{t+\Delta t} = \tilde{\mathbf{x}}_i^{t+\Delta t} + \mathbf{d}_i^{t+\Delta t}\alpha_i = \tilde{\mathbf{x}}_i^{t+\Delta t} + \frac{\Delta t^2}{m_i}\mathbf{F}_i \tag{13}$$

and thus

$$\mathbf{F}_i = \frac{m_i}{\Delta t^2}\mathbf{d}_i^{t+\Delta t}\alpha_i \tag{14}$$

which shows that by applying $\mathbf{F}_i$ to the contact point, the proposed collision-free position $\mathbf{x}_i^{t+\Delta t}$ is immediately reached. Penalty methods, in contrast, require in general several simulation steps to resolve a collision.

If Verlet is used as numerical integration scheme, then the obtained position is exact, otherwise it is still a very good approximation. Recently, Becker et al. [BGT06] have shown that similar exact formulations can also be derived for other numerical integration schemes.

3.3.3 Force equilibrium

To illustrate that the proposed contact forces $\mathbf{F}_i$ sum to 0 and thus ensure a global force equilibrium, we introduce local forces $\mathbf{f}_i$ and $\mathbf{f}_{T_i}$ for a collision (i, T_i). By showing that the local forces forces sum to 0 and that the local forces acting on a single point sum to $\mathbf{F}_i$, we conclude that the contact forces sum to 0.

Claim: Having a collision (i, T_i), the local force

$$\mathbf{f}_i = c_i \frac{m_i}{\Delta t^2}\mathbf{d}_i^{t+\Delta t}\alpha_i \tag{15}$$

on the point i and the local force

$$\mathbf{f}_{T_i} = \sum_{j=1}^{n} c_j h_{ij} \frac{m_j}{\Delta t^2}(-\mathbf{d}_i^{t+\Delta t})(1-\alpha_i). \tag{16}$$

on the triangle T_i ensure a local force equilibrium. Further, the sum of the local forces per point yields the proposed contact force $\mathbf{F}_i$ on that point.

Proof: For the local force equilibrium, we have

$$\begin{aligned} &\mathbf{f}_i + \mathbf{f}_{T_i} = \\ &= \frac{1}{\Delta t^2}(c_i m_i \mathbf{d}_i^{t+\Delta t}\alpha_i + \sum_{j=1}^{n} c_j h_{ij} m_j (-\mathbf{d}_i^{t+\Delta t})(1-\alpha_i)) \\ &= \frac{1}{\Delta t^2}\mathbf{d}_i^{t+\Delta t}(c_i m_i \alpha_i - \sum_{j=1}^{n} c_j h_{ij} m_j (1-\alpha_i)) \end{aligned} \tag{17}$$

Using the definition of α_i (5), we get

$$\mathbf{f}_i + \mathbf{f}_{T_i} = 0 \tag{18}$$

Notice that since the local force equilibrium is a mandatory requirement, the expression for α_i as proposed in (5) is obtained by solving (17) for α_i.

Since we have shown that for a collision (i, T_i), the local forces sum to zero, it follows that the sum of local forces over all collisions is also zero. We show now that by summing up all local forces per point, we yield the contact force $\mathbf{F}_i$. It follows that the contact forces sum to zero, as required by (2).

To calculate the contact force $\mathbf{F}_i$ per point, we need to consider the coupling of contacts. Thus, we sum over all contacts:

$$\begin{aligned} \sum_{i\in C}(\mathbf{f}_i + \mathbf{f}_{T_i}) &= \frac{1}{\Delta t^2}\sum_{i\in C}\Big(c_i m_i \alpha_i \mathbf{d}_i^{t+\Delta t} + \\ &\quad + \sum_{j=1}^{n} c_j h_{ij} m_j (-\mathbf{d}_i^{t+\Delta t})(1-\alpha_i)\Big) \end{aligned} \tag{19}$$

Using the assumption (3) for the penetration depths $\mathbf{d}_i^{t+\Delta t}$ and α_i, we get

$$= \frac{1}{\Delta t^2}\sum_{i\in C}\Big(c_i m_i \alpha_i \mathbf{d}_i^{t+\Delta t} + \sum_{j=1}^{n} c_j h_{ij} m_j \mathbf{d}_j^{t+\Delta t}\alpha_j\Big) \tag{20}$$

Reordering for the index i yields

$$\begin{aligned} &= \frac{1}{\Delta t^2}\sum_{i\in C}\Big(c_i m_i \alpha_i \mathbf{d}_i^{t+\Delta t} + \sum_{j=1}^{n} c_i h_{ji} m_i \alpha_i \mathbf{d}_i^{t+\Delta t}\Big) \\ &= \frac{1}{\Delta t^2}\sum_{i\in C} c_i m_i \alpha_i \mathbf{d}_i^{t+\Delta t}(1 + \sum_{j=1}^{n} h_{ji}) \end{aligned} \tag{21}$$

And by using the definition of c_i

$$\sum_{i\in C}(\mathbf{f}_i + \mathbf{f}_{T_i}) = \sum_{i\in C}\underbrace{\frac{m_i}{\Delta t^2}\alpha_i \mathbf{d}_i^{t+\Delta t}}_{=\mathbf{F}_i} = \sum_{i\in C}\mathbf{F}_i = 0 \tag{22}$$

We have shown that by reordering the terms in the sum of local forces over all collisions (left hand side of (22)), we arrive at the sum of contact forces over all collisions (right hand side of (22)), which conforms to the sum of

contact forces over all contact points. Thus the sum of local forces acting on a single contact point is

$$\mathbf{F}_i = \frac{m_i}{\Delta t^2}\alpha_i \mathbf{d}_i^{t+\Delta t} \tag{23}$$

as claimed in (4). As a consequence, the proposed contact forces $\sum_{i\in C}\mathbf{F}_i$ sum to zero and thus ensure a global force equilibrium.

□

In (21), we have neglected the fact that points $j \in T_i$ do not necessarily collide themselves and thus cannot be reordered for an $i \in C$. However, a contact force for these boundary points is easily derived such that both local and global force equilibrium are met. The details are omitted due to lack of space.

3.4 Frictional contacts

To implement frictional contacts, a force component orthogonal to $\mathbf{F}_i$ is computed using Coulomb's law [MC94]. This force component is then added to the contact force $\mathbf{F}_i$. Similar to [PPG04], we assume that frictional forces do not induce significant deformations. This allows us to decouple friction from the contact force computation.

3.5 Discussion

We showed how to derive a contact force per point such that for all contact points, a collision-free state is yielded.

We proposed a way to compute the contact forces analytically, i. e. without employing iterative solvers. This is made possible since we assumed a one-dimensional contact space per collision (i, T_i), i. e. we assumed that the penetration depths of the vertices $j \in T_i$ conform to the penetration depth of the point i. This is obviously not the case for general configurations. However, the differences $\varepsilon_{ij} = \mathbf{d}_i^{t+\Delta t} + \mathbf{d}_j^{t+\Delta t}$ approach zero if the angles between triangles adjacent to i and T_i approach zero. Thus, the differences ε_{ij} can be made arbitrary small by employing sufficiently densely sampled meshes.

Due to the approximation errors, the sum of contact forces is not exactly zero, contradicting the law of energy conservation. In the implementation, these ghost forces are eliminated by computing the ε_{ij} and correcting the contact force per contact point. These corrections are computed in constant time.

The small overlaps that result from the approximations made in the derivation of a collision-free state in Sec. 3.3.1 are hardly noticeable in interactive simulations. Moreover, they do not induce a violation of the laws of energy conservation.

4 IMPLEMENTATION

We have integrated our approach into a simulation framework for deformable objects, sketched in Algorithm 1. To compute the deformations, linear and non-linear finite element methods, and a mass-spring deformable model have been employed. In fact, our approach treats the computation of deformations as a black box process.

repeat
  $\mathbf{p} \leftarrow \text{ComputeDeformation}(\mathbf{x}^t)$;
  $\mathbf{p} \leftarrow \mathbf{p} + \text{ComputeGravity}$;
  $\tilde{\mathbf{x}}^{t+\Delta t} \leftarrow \text{UnconstrainedMotion}(\mathbf{x}^t, \mathbf{v}^t, \mathbf{p})$;
  $C \leftarrow \text{DetectCollisions}(\tilde{\mathbf{x}}^{t+\Delta t})$;
  $\mathbf{d}^{t+\Delta t} \leftarrow \text{ComputePenetrationDepths}(C, \tilde{\mathbf{x}}^{t+\Delta t})$;
  $\mathbf{F} \leftarrow \text{ComputeContactForces}(C, \mathbf{x}^t, \tilde{\mathbf{x}}^{t+\Delta t}, \mathbf{d}^{t+\Delta t}, \mathbf{p})$;
  $\mathbf{x}^{t+\Delta t} \leftarrow \text{ConstrainedMotion}(C, \mathbf{x}^t, \mathbf{v}^t, \mathbf{p}^t + \mathbf{F})$;
  $t \leftarrow t + \Delta t$;
until stop;

Algorithm 1: Overview of the simulation framework. Here, $\mathbf{x}^t$, $\mathbf{v}^t$ and $\mathbf{p}^t$ are the positions, velocities and internal forces on the points in the current time step. The positions $\tilde{\mathbf{x}}^{t+\Delta t}$ result from unconstrained motion, and C is the set of colliding points.

After the forces on the points have been computed, the objects are evolved in time, assuming a Newtonian second order world. Both explicit and implicit integration schemes have been tested, and we found that the explicit Verlet scheme [Ver67] provides a good ratio of accuracy and efficiency. The free motion of the objects results in an eventually colliding state.

To detect collisions of the unconstrained positions, we employ an algorithm based on spatial hashing [THM*03]. Further, the penetration depth $\mathbf{d}_i^{t+\Delta t}$ of each collided point is computed [HTK*04], yielding the contact space.

We then compute contact forces in the contact space that accelerate the points immediately to their collision-free positions. Thus the previous free motion is corrected.

5 RESULTS

We tested our implementation on various problems, ranging from complex off-line computations to interactive animations. In this discussion, we focus on three main aspects: Collisions of objects with locally differing elasticities and stress, challenging resting states, and performance measurements in massive scenarios. All experiments have been performed on an Intel Xeon PC, 3.8 GHz using an nVidia Quadro FX 4500 graphics card.

Locally differing elasticities. The proposed approach computes response forces per contact point by maintaining a local force equilibrium. Thus, the collision-free position of the contact point is directly governed by the elasticities of the neighboring elements. In addition, the method comes with no user-defined parameters, therefore collision configurations with temporally and spatially varying stress can be consistently handled. In Fig. 3 on the left, elastic bars are squeezed between two fixed anchors and thus they are deformed. Due to the low elasticities of the bars

(Young modulus 100kN/m^2), the stress on the contact regions is enormous high. Nevertheless, a collision-free state is maintained. In Fig. 3 right, the two bars (Young modulus 5000kN/m^2) deform a softer cube (Young modulus 30kN/m^2). The deformations are computed by employing non-linear finite element methods based on the Green-Lagrange stress tensor, showing that our response approach can also handle non-linear deformations. Further, in contrast to [GOM*06], the performance of the collision response is not affected by the elasticities of the contact regions.

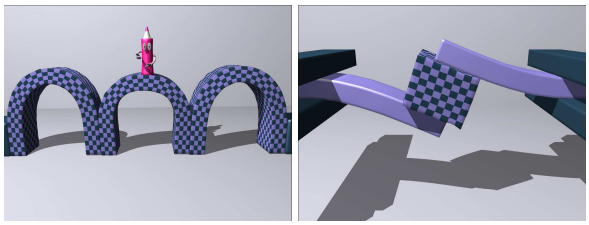

Figure 3: Left: Elastic bars are squeezed between anchors. A collision-free state is maintained even if the stresses on the contact regions are enormous high. Right: A soft cube is deformed by stiff bars. To compute the deformation, non-linear finite element methods have been employed.

Frictional contacts. The 'archway' (Fig. 4) is a classical problem in architecture. In fact, this construction can be built without employing any gluing substance. Its stability relies on a combination of pressure and static friction that prevents the elements from sliding off each other. We are able to simulate a stable resting state of the 'archway' even if its equilibrium is disturbed by objects falling onto it. Each wedge-shaped element consists of 375 tetrahedra, has a Young modulus of 20kN/m^2, a Poisson ratio $\nu = 0.35$, and a static friction coefficient of 0.95. The simulation runs at 40 frames per second in average, including deformation, collision detection and response, and visualization.

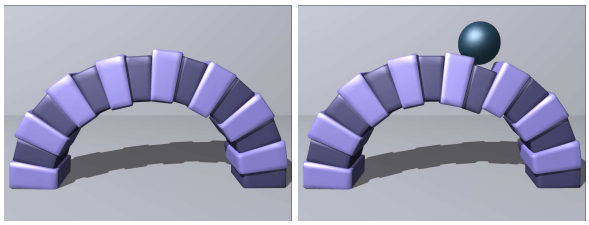

Figure 4: Simulation of a classical problem in architecture. The sensitive equilibrium of static friction and pressure makes this configuration a challenge for the collision response. Each element consists of 375 tetrahedra. The simulation runs at 40 frames per second, and there are 400 contact points in average.

Performance. The complexity of our response scheme is linear in the number of contact points. We performed an experiment with 500 objects being dropped into a container (see Fig. 5). Each object has a

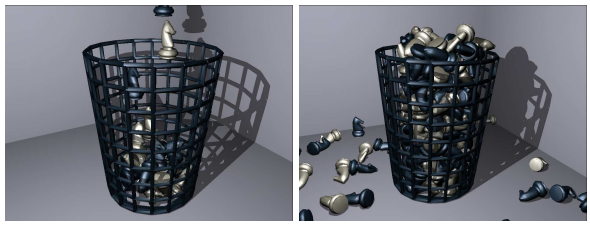

Figure 5: To test the performance of the scheme, 500 deformable chess figures are filled into a container. Thus the number of collisions grows linearly in time.

Young modulus of 10kN/m^2. The total number of mass points is 50.4K, and the total number of tetrahedrons is 88.2K. Fig. 6 indicates that the time to perform the collision response linearly depends on the number of collisions.

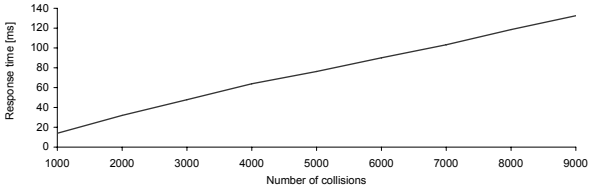

Figure 6: The measurements indicate that the performance of the proposed approach is linear in the number of collisions.

Fig. 1 illustrates the simulation of 200 chained torii falling onto an elastic membrane. The membrane deforms and buckles under the weight of the chain, but nevertheless a stable resting state is reached. The overall number of tetrahedrons is 80K, and there are 2500 contacts in average. The computation of one simulation pass takes 470ms in total, and the collision response alone takes 41ms.

6 CONCLUSION

We have presented a novel approach to handle collisions of deformable objects. The approach combines the benefits of penalty and constraint methods: We compute the positions of the colliding points on the contact surface by considering the stress on each point. A contact force is then computed that accelerates the point to this constrained position in the subsequent simulation step, thus a collision-free state is maintained. In contrast to penalty methods, the approach comes with no user-defined force constant. Therefore, the intrinsic problem to choose a constant that does not overshoot but resolves the collision is avoided. In contrast to constraint methods, the resulting system of equations can be decoupled and thus solved analytically, without employing iterative numerical methods. As a consequence, the approach is easy to implement and less vulnerable to numerical problems. Further, it requires only a small and constant number of operations per contact point.

The robustness of the approach depends on the computed penetration depths [HTK*04]. For deep intersec-

tions, this scheme is subject to fail, and the objects cannot be separated.

Currently, we are working on an extension of the proposed scheme to respond to self-collisions. This allows for handling collisions of non-volumetric deformable models such as cloth or hair.

REFERENCES

[Bar89] Baraff D.: Analytical methods for dynamic simulation of nonpenetrating rigid bodies. in Computer Graphics (Proc. Siggraph) (1989), vol. 23, pp. 223–232.

[BGT06] Becker M., Gissler M., Teschner M.: Local constraint methods for deformable objects. in Third Workshop in Virtual Reality, Interactions and Physical Simulations (2006). to appear.

[BW92] Baraff D., Witkin A.: Dynamic simulation of non-penetrating flexible bodies. Computer Graphics (Proc. Siggraph) 26, 2 (1992), 303–308.

[CW05] Cirak F., West M.: Decomposition contact response (DCR) for explicit finite element dynamics. International Journal for Numerical Methods in Engineering 64, 8 (2005).

[DAK04] Duriez C., Andriot C., Kheddar A.: Signorini's contact model for deformable objects in haptic simulations. in IEEE/RSJ International Conference on Intelligent Robots and Systems (2004), pp. 3232–3237.

[DDCB01] Debunne G., Desbrun M., Cani M.-P., Barr A. H.: Dynamic real-time deformations using space and time adaptive sampling. in Proc. Siggraph (2001), pp. 31–36.

[DDKA06] Duriez C., Dubois F., Kheddar A., Andriot C.: Realistic haptic rendering of interacting deformable objects in virtual environments. IEEE Transactions on Visualization and Computer Graphics 12, 1 (2006), 36–47.

[DMG05] Dequidt J., Marchal D., Grisoni L.: Time-critical animation of deformable solids. Computer Animation and Virtual Worlds 16, 3–4 (2005), 177–187.

[Gas93] Gascuel M. P.: An implicit formulation for precise contact modeling between flexible solids. in Computer Graphics (Proc. Siggraph) (1993), pp. 313–320.

[GOM*06] Galoppo N., Otaduy M. A., Mecklenburg P., Gross M., Lin M. C.: Fast simulation of deformable models in contact using dynamic deformation textures. in Proc. Eurographics/ACM Siggraph Symposium on Computer Animation (2006), pp. 73–82.

[HFS03] Hirota G., Fisher S., State A.: An improved finite-element contact model for anatomical simulations. in The Visual Computer, vol. 19. Springer, 2003, pp. 291–309.

[Hig96] Higham N. J.: Accuracy and Stability of Numerical Algorithms. Society for Industrial and Applied Mathematics, Philadelphia, PA, USA, 1996.

[HSO03] Hauser K. K., Shen C., O'Brien J. F.: Interactive deformation using modal analysis with constraints. in Graphics Interface (2003), pp. 247–256.

[HTK*04] Heidelberger B., Teschner M., Keiser R., Mueller M., Gross M.: Consistent penetration depth estimation for deformable collision response. in Proc. Vision, Modeling, Visualization (2004), pp. 339–346.

[JP02] James D., Pai D.: DyRT: Dynamic response textures for real time deformation simulation with graphics hardware. ACM Transactions on Graphics 21, 3 (2002), 582–585.

[KEP05] Kaufman D. M., Edmunds T., Pai D. K.: Fast frictional dynamics for rigid bodies. ACM Transactions on Graphics 24, 3 (2005), 946–956.

[KMH*04] Keiser R., Müller M., Heidelberger B., Teschner M., Gross M.: Contact handling for deformable point-based objects. in Proc. Vision, Modeling, Visualization (2004), pp. 339–347.

[MC94] Mirtich B., Canny J. F.: Impulse-Based Dynamic Simulation. Tech. Rep. UCB/CSD-94-815, EECS Department, University of California, 1994.

[Mor88] Moreau J. J.: Unilateral contact and dry friction in finite freedom dynamics. No. 302. 1988, pp. 1–82.

[MW88] Moore M., Wilhelms J.: Collision detection and response for computer animation. Computer Graphics (Proc. Siggraph) 22, 4 (1988), 289–298.

[NMK*05] Nealan A., Müller M., Keiser R., Boxermann E., Carlson M.: Physically Based Deformable Models in Computer Graphics. in Eurographics-STAR (2005), pp. 71–94.

[PPG04] Pauly M., Pai D. K., Guibas L. J.: Quasi-rigid objects in contact. in Proc. Eurographics/ACM Siggraph Symposium on Computer Animation (2004), pp. 109–119.

[ST05] Spillmann J., Teschner M.: Contact surface computation for coarsely sampled deformable objects. in Proc. Vision, Modeling, Visualization (2005), pp. 289–296.

[THM*03] Teschner M., Heidelberger B., Müller M., Pomerantes D., Gross M. H.: Optimized spatial hashing for collision detection of deformable objects. in Proc. Vision, Modeling, Visualization (2003), pp. 47–54.

[TKH*05] Teschner M., Kimmerle S., Heidelberger B., Zachmann G., Raghupathi L., Fuhrmann A., Cani M.-P., Faure F., Magnenat-Thalmann N., Strasser W., Volino P.: Collision Detection for Deformable Objects. Computer Graphics Forum 24, 1 (2005), 61–81.

[TPBF87] Terzopoulos D., Platt J., Barr A., Fleischer K.: Elastically deformable models. Computer Graphics (Proc. Siggraph) 21, 4 (1987), 205–214.

[Ver67] Verlet L.: Computer experiments on classical fluids. Ii. equilibrium correlation functions. Physical Review 165 (1967), 201–204.

[VMT00] Volino P., Magnenat-Thalmann N.: Accurate collision response on polygonal meshes. in Proc. Computer Animation (2000), IEEE Computer Society, pp. 154–163.